NREL/CP-530-23580 • UC Category: 1250

The Morphology of CdS Thin Films Deposited on SnO_2-Coated Glass Substrates

F.S. Hasoon, M.M. Al-Jassim,
A. Swartzlander, P. Sheldon, A.A.J. Al-Douri,
and A.A. Alnajjar

Presented at the 26th IEEE Photovoltaic Specialists Conference, September 29B October 3, 1997, Anaheim, California

National Renewable Energy Laboratory
1617 Cole Boulevard
Golden, Colorado 80401-3393
A national laboratory of
the U.S. Department of Energy
Managed by Midwest Research Institute
for the U.S. Department of Energy
under contract No. DE-AC36-83CH10093

Prepared under Task No. PV707202

September 1997

THE MORPHOLOGY OF CdS THIN FILMS DEPOSITED ON SnO_2-COATED GLASS SUBSTRATES

F. S. Hasoon, M. M. Al-Jassim, A. Swartzlander, and P. Sheldon
National Renewable Energy Laboratory, Golden, CO 80401, USA
A. A. J. Al-Douri and A. A. Alnajjar
Dept. of Physics, United Arab Emirates University, Al Ain, UAE

ABSTRACT

The morphology and microstructure of cadmium sulfide (CdS) thin films are a major concern in the fabrication process of CdTe solar cells. In this work, we investigate the morphology and microstructure of chemical-bath-deposited CBD CdS in order to better understand the growth conditions that give rise to films for optimum device performance. The film morphology was investigated by field-emission, high-resolution scanning electron microscopy (SEM). The film microstructure was studied by transmission electron microscopy (TEM), while the film's chemistry was investigated by Auger electron spectroscopy (AES). All films examined exhibited pinholes and discontinuities varying in size and density. This may have a significant impact on cell performance by providing shunt paths between the CdTe and the SnO_2. Additionally, the CdS films are heavily faulted, which may partially explain why a high density of planar defects is observed in the CdTe/CdS interface region.

INTRODUCTION

Thin films of CdS have been used as junction partners in CdTe and $CuInSe_2$ solar cells for many years. The best cell performance has been achieved using CdS films grown by chemical-bath deposition (CBD) rather than by other methods, such as physical-vapor deposition, or close-spaced sublimation. However, limited investigations have been performed on the morphology and microstructure of these films [1-7]. These parameters are believed to be particularly important to CdTe cell technology. This is due to the fact that CdS acts as a substrate for the subsequent growth of CdTe films, and also acts as a window layer in the backwall cell configuration. Therefore, it is important to achieve the following in order to optimize the CdS films:

1. To avoid shunting, the film must be continuous, and free of voids, large particles, and discontinuities.

2. In order to minimize optical losses due to absorption, the CdS film should have the minimum possible thickness.

3. The film's microstructure must have minimal density of crystalline defects, as it was shown [4] that structural defects such as stacking faults and twins propagate from the CdS into the CdTe.

In this work, we investigate the morphology, chemistry, and microstructure of CBD-deposited CdS in order to better understand the growth conditions that give rise to films for optimum device performance.

EXPERIMENTAL

The CdS films used in this study were deposited by CBD using a solution of ammonium acetate, cadmium acetate, thiuorea and ammonium hydroxide in de-ionized water. The solution was basic, with a pH ~10. Further, a solution temperature of 90°C was used, while the substrates were SnO_2-coated glass. The SnO_2:F, which is a transparent conducting oxide acting as a front contact, was deposited by chemical-vapor deposition. For each CdS deposition, the substrates were removed from the solution at different times in order to obtain films with different thicknesses. The film thickness in this study was varied from 15 to 100 nm by varying the deposition time from 10 to 40 min.

The film morphology was investigated by field-emission, high-resolution scanning electron microscopy (FESEM). The film microstructure was studied by TEM, while the film chemistry was examined by Auger electron spectroscopy (AES) and back-scattered SEM imaging. Additionally, the morphology of the SnO_2-coated glass substrates was investigated in order to study the SnO_2 surface prior to the deposition of CdS.

RESULTS

FESEM examinations of these films clearly revealed their surface structure. Two types of grains were observed (Fig. 1). The first type has a size in the 100-200 nm range. Suprimposed on this are smaller grains having a grain size in the 30-60 nm range. Detailed comparison of the surfaces of the SnO_2 prior to CdS deposition and those of CdS films revealed that the larger grains correspond to the underlying SnO_2, while the smaller grains correspond to the CdS films. The CdS grain size was studied as a function of film thickness. Fig. 1 shows a CdS film deposited for 15 min, resulting in a film thickness of approximately 30 nm. The average grain size in this film is approximately 30 nm, which corresponds to the film thickness. However, increasing the film thickness to 100 nm did not give rise to a linear increase in grain size. This is illustrated in Figure 2 which is a FESEM micrograph of a 100-nm thick film, exhibiting an average grain size of 60 nm.

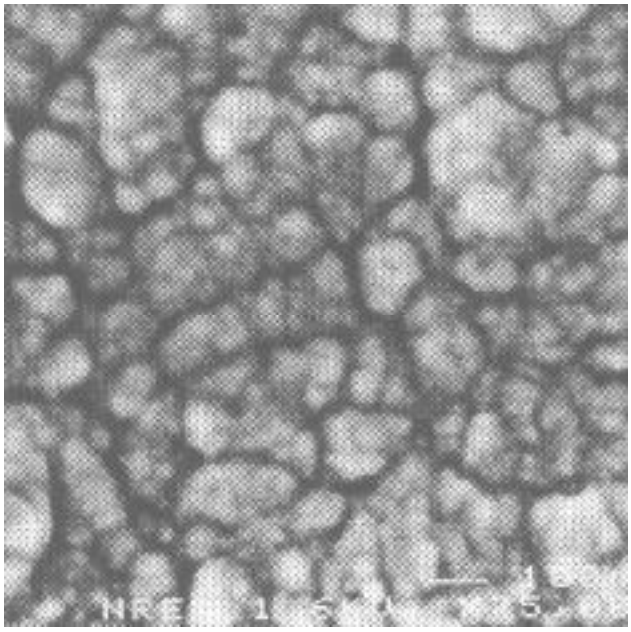

Fig. 1. FESEM micrograph of a 30-nm thick CdS film showing an average grain size of ~ 30 nm.

Increasing the deposition time beyond 40 min did not give rise to thicker films. However, it resulted in markedly different surface morphology, as much finer grains than those in Fig. 2 were observed. This is believed to be caused by the homogeneous nucleation of CdS particles within the growth solution and their subsequent deposition on the film surface. In addition to investigating films with longer growth time, the effects of annealing on film morphology was studied. In the first experiment, a CdS film was annealed at 400°C for 5 min in hydrogen ambient to simulate the effect of our standard heat treatment prior to the deposition of CdTe. No significant effects were observed on the film's surface. In the second experiment, we repeated the above- mentioned heat treatment, and subsequently increased the film temperature to 600°C to simulate the temperature profile during a typical CdTe-deposition run. As soon as that temperature was reached, the run was aborted and the film was cooled down and examined. Fig. 3 shows that the surface of such a film exhibits a significant deterioration. Although some evidence of recrystallization is seen, such a film has a much higher surface roughness and exhibits a higher density of pinholes. The latter are believed to be caused by the re-evaporation of part of the film. It must be mentioned here, however, that presently we are unable to determine whether the deterioration takes place during the temperature ramp up or ramp down.

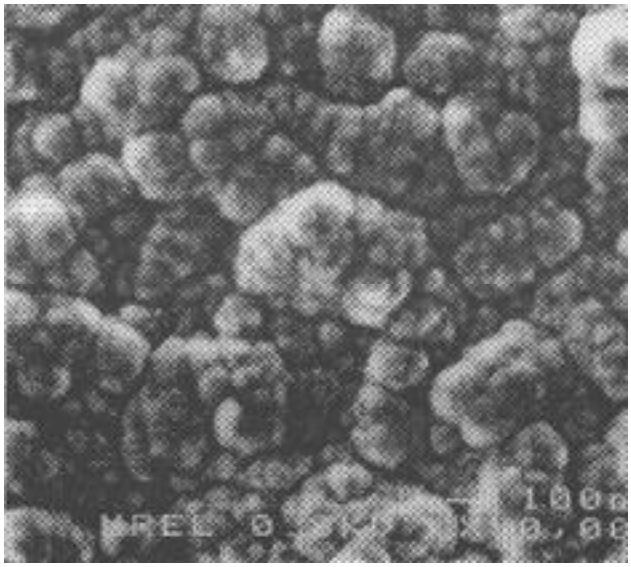

Fig. 2. FESEM micrograph of a 100-nm thick CdS film, showing an average grain size of ~60 nm.

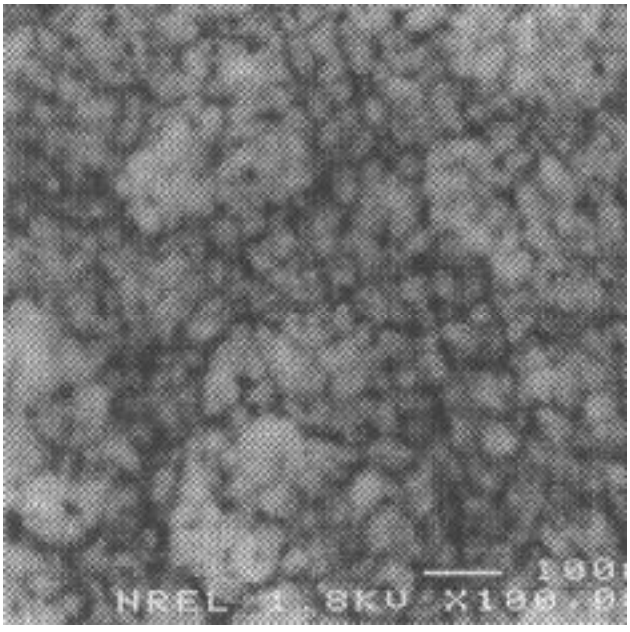

Fig. 3 FESEM micrograph of a CdS film after heat treatment.

Particular emphasis was placed in this study on the continuity of the CBD CdS films. Examining the thinnest sample (10-min. deposition, 20-nm film) indicated that large areas of the SnO_2 film are covered by CdS. However, the coverage is not complete. Increasing the deposition time to 15 min resulted in a higher surface coverage. Nonetheless, two undesirable features were clearly revealed by FESEM. The first is gross discontinuities in the CdS film, and the second is a high density of pinholes (Fig. 4). The size of the gross discontinuities observed was up to 20 μm. What we refer to as pinholes here, however, are features of the order of a micron or less.

As the deposition time increased, both the size of the discontinuities and their density decreased. At 30 min of deposition, the large discontinuities shrunk in size to the 1-2 μm range and the density of the pinholes decreased significantly. At 35 min of deposition, the film thickness is ~100 nm. The gross film discontinuities are virtually absent, but pinholes are still clearly evident. Increasing the deposition time to 40 min or beyond resulted in undesir-

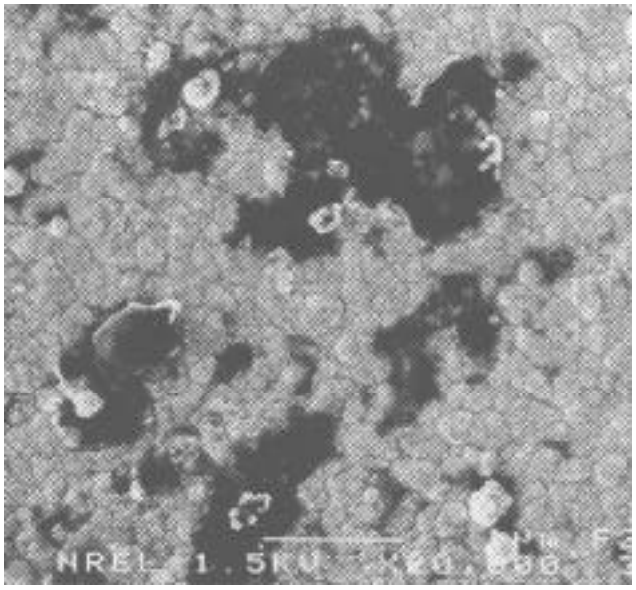

Fig. 4 FESEM micrograph of a 40-nm thick CdS film, showing discontinuities and pinholes.

able film properties, such as the deposition of fine grain material on the film's surface and the incorporation of particles in the film. The latter are believed to be caused by homogeneous nucleation of CdS in the solution.

The chemical properties of the gross discontinuities were investigated by AES. Such analysis revealed that many of these discontinuities are bare SnO_2 film. This is indicative of the lack of CdS nucleation in these areas. The nucleation could have been inhibited by the contamination of these areas on the SnO_2 film surface. Other AES analyses showed that some of these areas comprise a thinner CdS film than the matrix. This is clearly shown in Fig 5, which shows AES survey taken within one of these regions. Before sputtering, the CdS signal is evident; however, after a short 1-min sputter, only the SnO_2 signal was detected from the defective region. This is clearly indicative of the low CdS film thickness in these regions. Furthermore, AES analyses revealed the presence of oxygen and carbon in many of these regions. This supports the hypothesis that this type of defect is caused by contamination. The latter is likely to originate from the impurity species in the chemical bath itself [8].

The compositional properties of the pinholes were probed by backscattered electron imaging (BSI) in the FESEM. Unlike secondary-electron imaging (SEI), which is primarily topographical, BSI is primarily compositional. However, although this technique is sensitive to differences in composition, it is qualitative. Furthermore, it provides no information on the chemical elements present in the area analyzed. Fig 6a and 6b are SEI and BEI images of the same area in a CdS film. The BEI unambiguously confirms that what appears to be topographical difference in the SEI image is also compositionally different.

The microstructure of as-deposited and annealed films was investigated by TEM and X-ray diffraction. The CdS

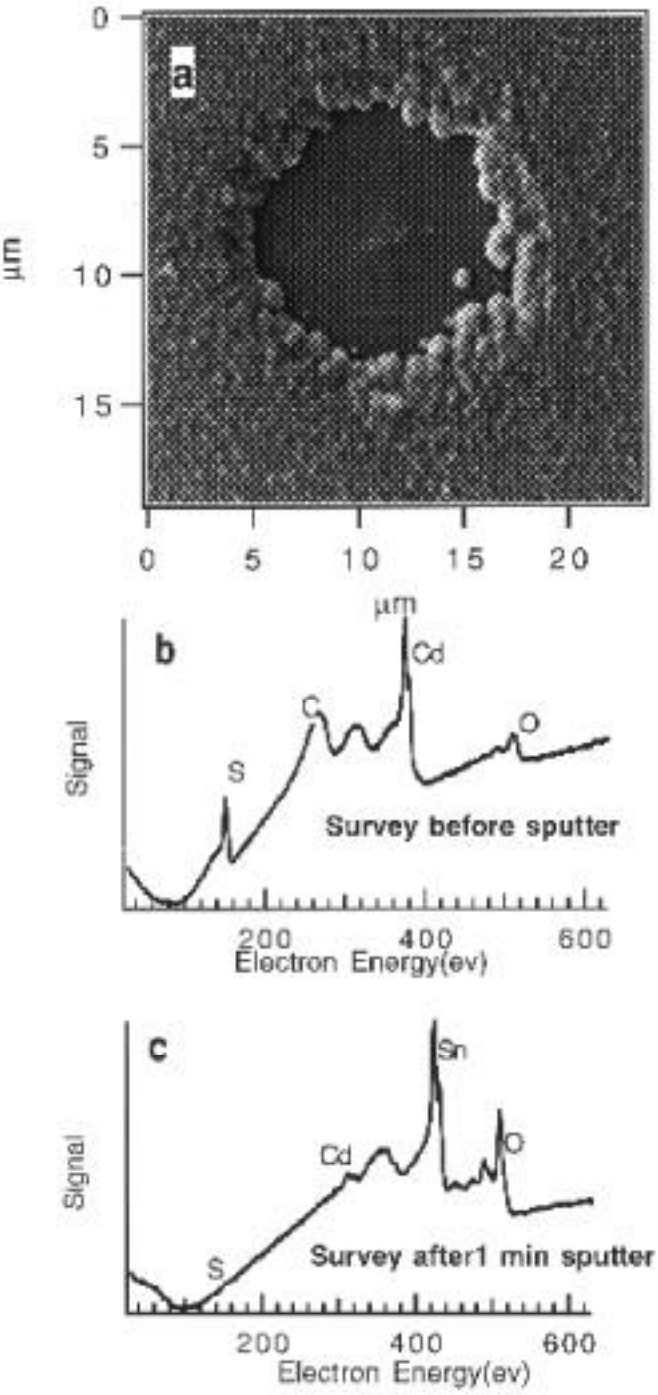

Fig. 5. (a) SEM image of a discontinuity in a CdS film, and AES surveys taken within one of these regions; (b) before and (c) after a short sputtering.

grains were heavily faulted. Most grains exhibited a high density of planar defects such as stacking faults. Furthermore, our 400°C, 5-min anneal had no effect on the defect density. XRD examination showed that the CdS has a hexagonal structure regardless of the film thickness or deposition conditions.

SUMMARY

In summary, all CdS films examined in this study exhibited pinholes and discontinuities varying in size and density. This could have a significant impact on cell performance as these pinholes may provide shunting paths between the CdTe and the SnO_2. Additionally, the CdS grains are heavily faulted, with a high density of stacking faults. This will have a deleterious effect on CdS/CdTe interface region, as we have shown in a previous study that planar defects in CdS tend to propagate into the CdTe films. Furthermore, the CdS films have a hexagonal crystal structure, which may explain why a high density of planar defects are generated at the CdS/CdTe interface, since CdTe is known to be cubic.

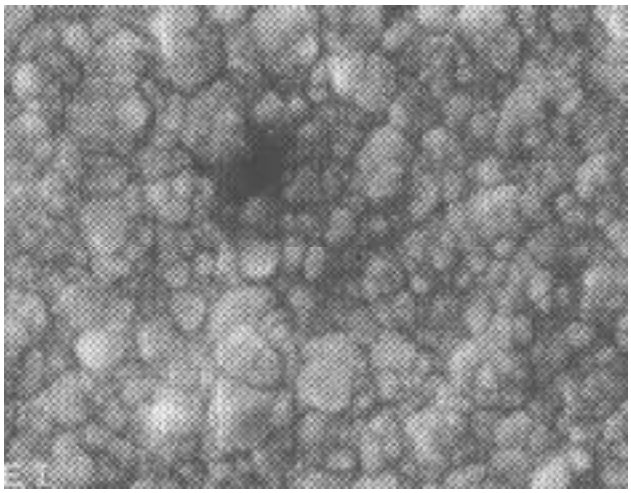

a

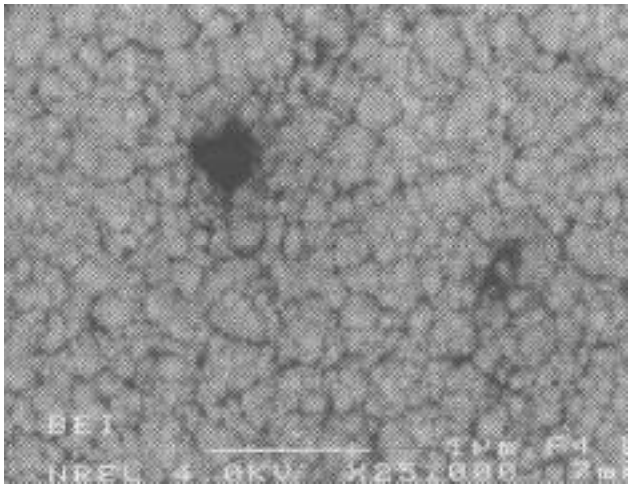

b

Fig. 6. (a) SEI and (b) BEI images of pinholes in a CdS film confirming the chemical difference between these regions and the CdS.

ACKNOWLEDGMENTS

The authors would like to acknowledge Kim Jones and Jay Riker of NREL for their contribution of the TEM and XRD data, respectively. This work was performed under the U.S. Department of Energy contract number DE-AC36-83CH10093.

REFERENCES

[1] R.L. Call, N.K. Jaber, K.Seshan, and J.R. Whyte, *Solar Energy Materials* **2**, 373 (1980).

[2] A. Mondal, T.K. Chaudhuri, and P. Pramanik, *Solar Energy Materials* **7**, 431 (1983).

[3] W.J. Danaher, L.E. Lyons, and G.C. Morris, *Solar Energy Materials* 1**2**, 137 (1985).

[4] M.M. Al-Jassim, F.S. Hasoon, K.M. Jones, B.M. Keyes, R.J. Matson, and H.R. Moutinho, Proc.23rd IEEE PVSC (IEEE, New York, 1993) p 459.

[5] H.R. Moutinho, R.G. Dhere, K. Ramanathan, P.Sheldon and L.L. Kazmesrski, Proc.25th IEEE PVSC (IEEE, New York, 1996) p 945.

[6] I.O. Oladeji and L. Chow, *J. Electrochem. Soc.* **144**, 2342 (1997).

[7] M.E. Ozsan, D.R. Johnson, M. Sadeghi, and D. Sivapathasundaram, *J. of Materials Science: Materials in Electronics* **7**, 119 (1996).

[8] A. Kylner, A. Rockett and L. Stolt, *Solid State Phenomena* **51**-**52**, 533 (1996).